

THE AB INITIO STUDY OF THE CATALYTIC HYDROGENATION OF THE OXIRENE

J.B. Mensah* and U.A. Kuévi

Laboratoire de Chimie Théorique et de Spectroscopie Moléculaire (L.A.C.THE.S.MO)
03 B.P. 3409 Cotonou, Bénin

(Received February 22, 2007; revised May 22, 2007)

ABSTRACT. The oxirene is an unsaturated heterocyclic molecule with one oxygen atom and two carbon atoms. Its hydrogenation has been performed on two catalytic site based on molybdenum disulfide (MoS_2) and tungsten disulfide (WS_2) of MoS_3H_3^+ and WS_3H_3^+ type, respectively. The calculations were carried out using the SCF and MP2 methods and B3LYP functional calculations. The results obtained showed that the hydrogenation of the oxirene is possible on these two kinds of catalytic sites on the one hand, and the reaction product is the acetaldehyde molecule, on the other hand. The reaction process study that led to the results showed that the catalytic hydrogenation of the oxirene is a dissociative process. On the basis of the variation of some parameters during the process, a mechanism of the reaction has been proposed.

KEY WORDS: Oxirene, Heterocyclic molecule, Hydrogenation, Molybdenum disulfide, Tungsten disulfide, Catalytic site, Acetaldehyde, Dissociative process

INTRODUCTION

The hydrogenation reaction is an important chemical process in the hydrotreating field. The molecules of which this reaction is carried out are heteroaromatic compounds like thiophene and its derivatives. That is why the hydrogenation reaction is often followed by the hydrogenolysis reaction. Various models have been proposed for active sites in hydrogenation and hydrogenolysis reaction on molybdenum sulfide catalyst [1-3]. The role played by edge and basal sites of the sulfide in both oxygen chemisorption and in hydrogenation is still moot although the question has been often investigated [4-6]. We have chosen to study the hydrogenation reaction of the oxirene using two catalytic site with three anionic vacancies based on molybdenum disulfide (MoS_2) and tungsten disulfide (WS_2) of MoS_3H_3^+ and WS_3H_3^+ type. The reaction coordinates used were the distance metal-oxygen and the distances carbon-hydrogen for the adsorption and the hydrogenation process, respectively.

EXPERIMENTAL

The calculation methods

The calculations methods are based on the Hartree-Fock (HF), the Møller-Plesset perturbation theory second-order correction to the Hartree-Fock energy (MP2) and the Density Functional Theory (DFT) [7-10]. In the Hartree-Fock method, the wave function is the functional of spin orbitals. The electronic energy of the ground state is obtained by applying the variation theorem.

In the Hartree-Fock theory, the energy has the form:

$$E_{HF} = V + \langle hP \rangle + \frac{1}{2} \langle PJ(P) \rangle - \frac{1}{2} \langle PK(P) \rangle$$

*Corresponding author. E-mail: menfolben@yahoo.fr

where V is the nuclear repulsion energy, P is the density matrix, $\langle hP \rangle$ is the one-electron (kinetic plus potential) energy, $\frac{1}{2} \langle PJ(P) \rangle$ is the classical coulomb repulsion of the electrons, and $-\frac{1}{2} \langle PK(P) \rangle$ is the exchange energy resulting from quantum (fermion) nature of electrons.

In the Møller-Plesset perturbation theory second-order correction to the Hartree-Fock energy (MP2) the functional of spin orbitals as for the Hartree-Fock theory is used. The energy has the form:

$$E_{MP2} = E_{HF} + E^{(2)}$$

where $E^{(2)}$ is the second-order correction.

In the DFT method, B3LYP is currently the most popular functional and uses a combination of the Local Spin Density Approximation (LSDA), Hartree-Fock (to give more predictive long range correlation), Becke's 3 parameter exchange functional and the Lee, Yang and Parr correlation. These are all combined as terms with three empirically defined coefficients. As such the calculations are longer than a Hartree-Fock but shorter than a MP2 perturbation calculation. The general opinion is that B3LYP calculations are nearer to experimental results than MP2 calculations because of the extensive optimization of their empirical content. The expression of energy E_{KS} based of Kohn-Sham method is:

$$E_{KS} = V + \langle hP \rangle + \frac{1}{2} \langle PJ(P) \rangle + EX_{[P]} + EC_{[P]}$$

where $EX_{[P]}$ is the exchange functional, and $EC_{[P]}$ is the correlation functional. The basis set used is lan12dz.

Calculation program

The calculations were performed with Gaussian-98W program [11]. The program data are the geometry of systems, their multiplicity and charge. The curves and the drawings of the system studied were performed with Excel and ChemDraw, respectively. The calculations were carried out in the "Laboratoire de Chimie Théorique et de Spectroscopie Moléculaire (LACTHESMO)" of "Université d'Abomey-Calavi" in Benin Republic.

Theoretical modelling of the hydrogenation process

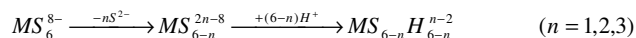
Modelling of the catalytic sites

Hydrotreated catalysts based upon molybdenum and tungsten sulfides are widely used. The structure of the catalysts has been studied and it is generally accepted that the active site of these catalysts consist of MoS_2 or WS_2 slabs in which the promoter atoms are incorporated [12-14]. The catalysts sites are generally viewed as anionic vacancies and results performed on molybdenum monocrystals support this general view [15, 16].

Different models for catalytic sites have been used in calculations based on quantum chemicals [17-20]. These studies involve mainly the hydrodesulfurization of thiophene and other molecules which are representative of the compounds present in the crude oil.

For the modelling studies performed in our laboratory, catalytic site with three anionic vacancies have been considered with the tungsten atom on the same model as this performed by Joffre *et al.* [21] who used the Hoffmann EHT method [22]. The principle of the creation on the anionic vacancies according to these authors consists to consider a cluster in the MoS_2 or WS_2 crystal containing one metal atom with degree of oxidation (+IV) surrounded by three sulfide ions S^{2-} . While eliminating one, two or three sulfide ions, one creates one, two or three anionic vacancies. In order to stabilize this system which carries charge (-VIII) protons are added. The

principle is illustrated by the Scheme I where $n = 2$ represents the charge of the site and in our present works $n = 3$.



Scheme I. Formation of n anionic vacancies.

Modelling of the hydrogenation reaction

The hydrogenation process has been performed from the optimized adsorptive geometry of the oxirene on the different site. This system being maintained fixed, the approach of the dihydrogen molecule has been carried out progressively (Figure 1). This reaction phase come to an end when all the system is optimized. The following phase of the process consists to move away the reaction product from the site what permit its optimization. The reaction coordinate during the hydrogenation phase is the C_9H_{13} distance and as far as the last phase is concerned, the reaction coordinate is the metal (site)-O distance (M_1O_8).

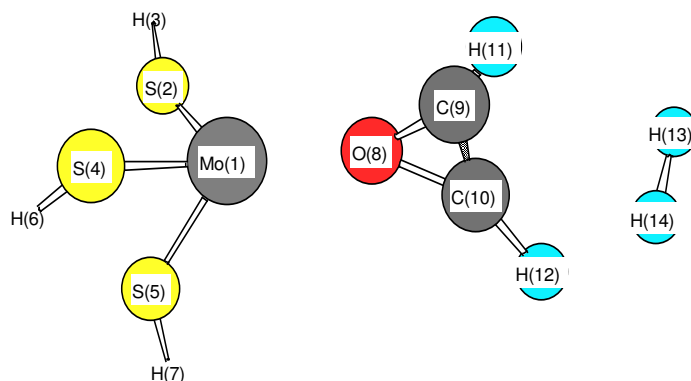


Figure 1. Scheme of the whole system studied (Mo can be changed into W and as well Mo as W can be designated by M).

RESULTS AND DISCUSSION

The reaction on $MoS_3H_3^+$ and $WS_3H_3^+$ catalytic sites

From the distance of 6 \AA to the each site, we have carried out the adsorption of the oxirene molecule using HF calculation. The M_1O_8 distance in the adsorptive optimized geometry is 1.981 \AA and 2.029 \AA for the $MoS_3H_3^+$ and $WS_3H_3^+$ catalytic sites, respectively (Figure 2).

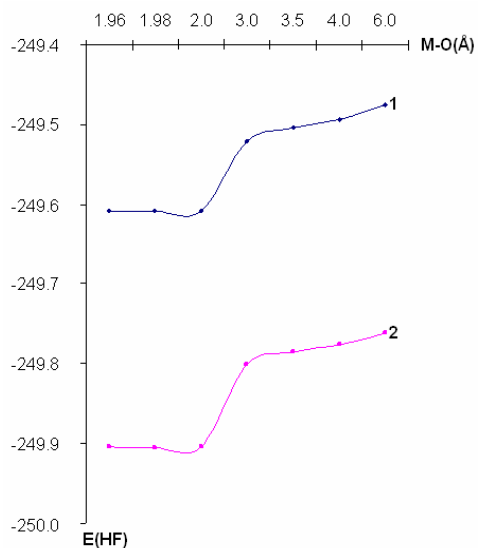


Figure 2. Adsorption of oxirene on MoS_3H_3^+ (1) and WS_3H_3^+ (2) catalytic sites.

The approach of the hydrogen molecule began at 4 Å from one of the carbon atom of the site-oxirene complex (C_9). The end of this phase of the process is characterised by the stabilisation of the system (Figure 3).

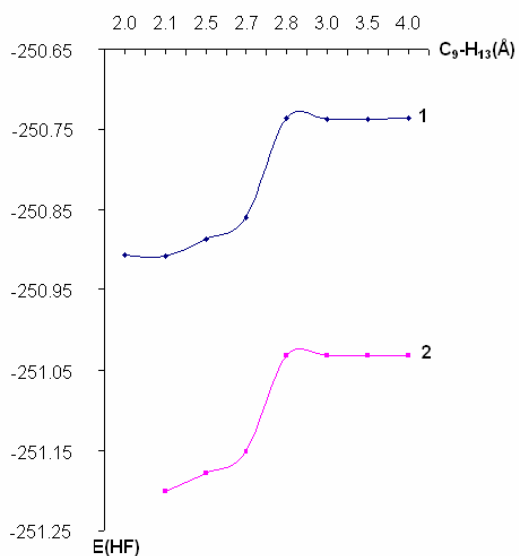


Figure 3. Hydrogenation of oxirene on the MoS_3H_3^+ (1) and WS_3H_3^+ (2) catalytic sites.

The geometric parameters of the new complex formed showed that the two hydrogen atoms (H_{13} and H_{14}) are fixed themselves on one of the two carbon atoms (C_{10}) followed by a slightly removal of the reaction product from the site. The last phase of all the process is the desorption of the reaction product which the geometry is optimized itself (Figure 4).

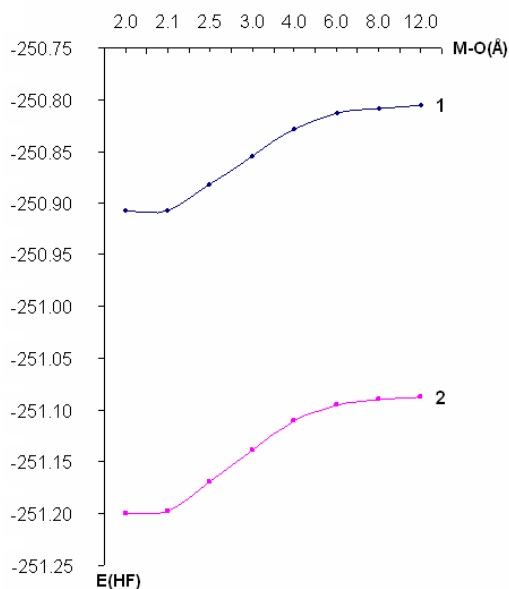


Figure 4. Desorption of the reaction product from the $MoS_3H_3^+$ (1) and $WS_3H_3^+$ (2) catalytic sites.

In the optimized adsorptive geometry of the complex site-oxirene, the slight difference concerning the distance metal-oxygen is the fact of the difference at the level of the radius of the two metallic atoms (1.39 Å (Mo), 1.40 Å (W)) [23].

During the adsorption of the oxirene on the two catalytic sites, the geometric parameters of the molecule have varied. It is matter of C_9O_8 , $C_{10}O_8$ and C_9C_{10} bonds whose length were initially 1.550 Å, 1.550 Å and 1.261 Å, respectively. In the adsorptive optimized geometry, C_9C_{10} bond is stretched (1.319 Å on $MoS_3H_3^+$ and 1.317 Å on $WS_3H_3^+$), on the one hand and the symmetry of the oxirene has been modified because of the stretch of the $C_{10}O_8$ bond (2.346 Å) and the shortening of the C_9O_8 bond (1.298 Å), on the other hand.

As far as the Mulliken population analysis is concerned, we have studied the charge on the metal (Mo and W) of the catalytic site, the oxygen atom and the two Carbon (C_9 and C_{10}) atoms. In the adsorptive optimized geometry of the system, the charges on the molybdenum and the tungsten atoms are positive and of same order of magnitude (0.570 a.u.). Concerning the oxygen atom, the negative charge has increased and has reached 0.76 a.u. When we consider the two carbon atoms, the charge is positive and the density of charge is higher on C_9 than on C_{10} . In the system, we noticed that the metal atom is an electrophilic center and the oxygen atom a nucleophilic center because of the electronegativity of the oxygen atom and the electropositivity of the metal atom.

The hydrogenation phase of the process is characterised by the variation of the bond length, the charges and the angles between bonds. The reaction coordinate used is the distance between

the carbon atom C_9 and the hydrogen atom H_{13} (C_9H_{13}). As far as the metal-oxygen distances are concerned, from 10 Å to optimized adsorptive geometry (2.1 Å), the Mo_1-O_8 and the W_1-O_8 distances are stretched out of 21.5 % and 16.40 %, respectively, passing from 1.981 Å to 2.407 Å on $MoS_3H_3^+$ and from 2.029 Å to 2.362 Å on $WS_3H_3^+$, what traduce a slightly removal of the oxirene molecule on which the hydrogen molecule seems to settle. As far as the C_9C_{10} bond is concerned, the length remains constant until 2.8 Å before its stretch followed by its shortening on the two sites. The final value of this bond length is 1.482 Å on $MoS_3H_3^+$ and 1.485 Å on $WS_3H_3^+$ which shows that on the two catalytic sites, it is the same results which are obtained. Concerning the C-O bonds, the C_9O_8 bond is shortened because the initial value is 1.298 Å and the final value 1.274 Å on $MoS_3H_3^+$ and 1.278 Å on $WS_3H_3^+$ while the length of $C_{10}O_8$ bond whose the length is in the start 2.346 Å is stretched and the final length is 2.407 Å at the end of the process confirming the tendency to the formation of aliphatic compound from the initial heterocyclic compound.

As far as the CH bonds are concerned, the length is the same and equal to 1.08 Å which shows that these bonds are all equivalent.

Concerning the angles, the values of angles $O_8C_9H_{11}$ (119.6°), $C_{10}C_9H_{11}$ (116.1°) and $C_{10}C_9O_8$ (124.3°) showed that the atoms C_{10} , C_9 , O_8 and H_{11} belong to the same plane because the sum of the angles values is equal to 360.0° . For the HCH angles, exactly the angles $H_{12}C_{10}H_{13}$, $H_{12}C_{10}H_{14}$ and $H_{13}C_{10}H_{14}$, the values are 107.30° , 109.50° and 109.50° , respectively and of which two of the values are close to the HCH angle value (109.28°) in the methyl group. The third angle differs from 1.98° compared with the previous value of HCH angle.

As far as the dihydrogen molecule is concerned, during the process, the length of the $H_{13}H_{14}$ bond has varied. On the two catalytic sites, the variation is the same and at the C_9H_{13} distance of 2.8 Å, the breaking of the bond intervened. In fact, the $H_{13}H_{14}$ bond length has increased in passing from 0.736 Å to 1.770 Å between 2.8 Å and 2.7 Å (Figure 5).

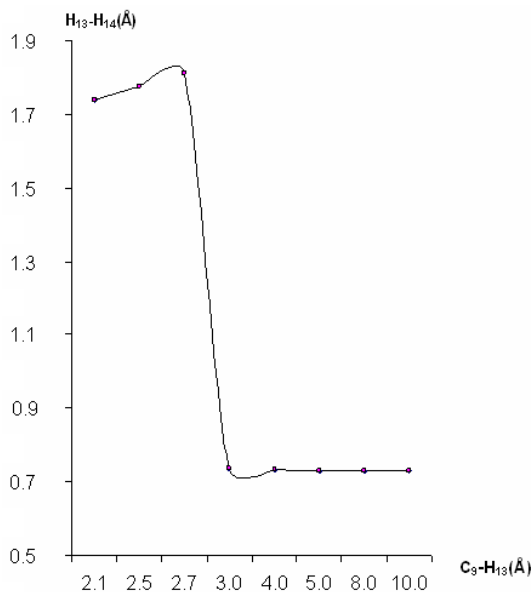


Figure 5. Variation of the dihydrogen molecule bond length ($H_{13}H_{14}$) during the hydrogenation process on the two catalytic sites.

During this process, the charge on each hydrogen atom is the same (+ 0.259 a.u.). These results showed that the hydrogenation of the oxirene molecule on the two kinds of catalytic site is a dissociative process.

In order to understand the mechanism of the reaction, we have calculated the initial energy of the system including the site-oxirene complex and the dihydrogen molecule, on the one hand, and the energy of the optimized geometry of all the system using the three calculation methods. The gap between the two types of energy corresponds to the energy of the reaction. The calculation results are summarised in the Tables 1 and 2.

Table 1. Energy of oxirene hydrogenation on MoS_3H_3^+ catalytic site.

Energy (au)					ΔE
Method	$\text{MoS}_3\text{H}_3^+ + \text{C}_2\text{H}_2\text{O}$	H_2	$\text{MoS}_3\text{H}_3^+ + \text{C}_2\text{H}_2\text{O} + \text{H}_2$	ΔE	($\text{kJ}\cdot\text{mol}^{-1}$)
HF	-249.60841	-1.12666	-250.90748	-0.17241	-452.23
MP2	-250.23605	-1.14391	-251.56801	-0.18805	-493.25
DFT	-251.90671	-1.17442	-253.26599	-0.18486	-484.89

$$\Delta E = E_{(\text{catalytic site} + \text{C}_2\text{H}_2\text{O} + \text{H}_2)} - E_{(\text{catalytic site} + \text{C}_2\text{H}_2\text{O})} - E_{(\text{H}_2)}$$

Table 2. Energy of oxirene hydrogenation on WS_3H_3^+ catalytic site.

Energy (au)					ΔE
Method	$\text{WS}_3\text{H}_3^+ + \text{C}_2\text{H}_2\text{O}$	H_2	$\text{WS}_3\text{H}_3^+ + \text{C}_2\text{H}_2\text{O} + \text{H}_2$	ΔE	($\text{kJ}\cdot\text{mol}^{-1}$)
HF	-249.90542	-1.12666	-251.20072	-0.16986	-445.54
MP2	-250.48893	-1.14391	-251.82088	-0.18804	-493.23
DFT	-252.19935	-1.17442	-253.55537	-0.18160	-476.34

$$\Delta E = E_{(\text{catalytic site} + \text{C}_2\text{H}_2\text{O} + \text{H}_2)} - E_{(\text{catalytic site} + \text{C}_2\text{H}_2\text{O})} - E_{(\text{H}_2)}$$

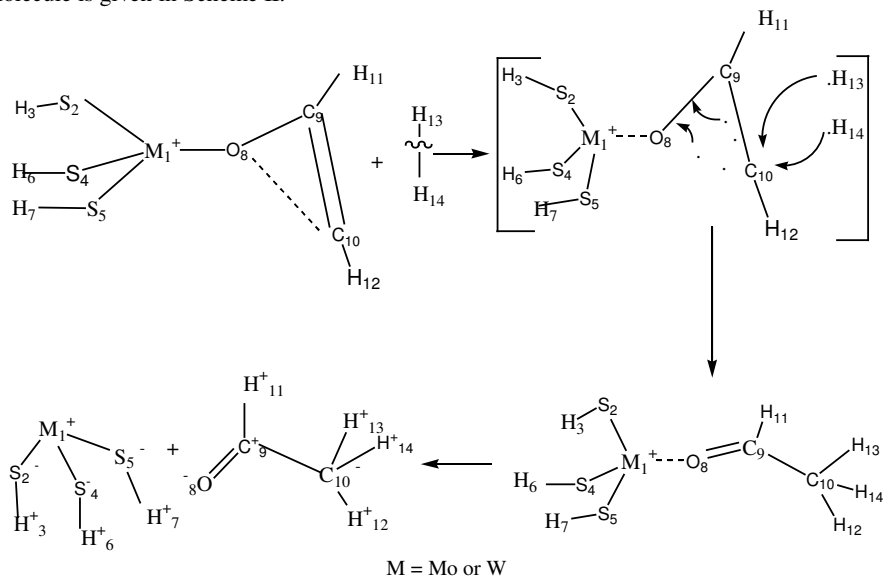
The data in the Tables 1 and 2 show that the MP2 calculation method leads to the most stable system. On the basis of the different parameters studied, the geometrical structure of the reaction product is that of the acetaldehyde molecule. This molecule can be obtained experimentally in the presence of basic or acidic and other metal oxide catalysts [24-27]. The formation of this molecule is the result of the dissociation of the dihydrogen molecule followed by the formation of two C-H bonds in the reactant molecule. Independently of the catalytic process, we have calculated the different energies which accompany the process according to the three calculation methods (Table 3).

Table 3. The calculated data of the dissociation of H-H bond and the formation of two C-H bonds.

Energy (au)			
System	HF	MP2	DFT
C	-37.59892	-37.63539	-37.78699
H	-0.49764	-0.49764	-0.49891
CH	-38.25955	-38.30361	-38.47784
H_2	-1.12666	-1.14391	-1.17442
Formation $\text{CH}(E_F)$ ($\text{H} + \text{C} \rightarrow \text{CH}$)	-0.16299	-0.17058	-0.19194
Dissociation $\text{H}_2(E_D)$ ($\text{H}_2 \rightarrow 2\text{H}$)	-0.13138 (-344.95 $\text{kJ}\cdot\text{mol}^{-1}$)	-0.14864 (-390.24 $\text{kJ}\cdot\text{mol}^{-1}$)	-0.17660 (-463.66 $\text{kJ}\cdot\text{mol}^{-1}$)
$E_D + 2E_F$	0.19460 (510.93 $\text{kJ}\cdot\text{mol}^{-1}$)	0.19253 (505.50 $\text{kJ}\cdot\text{mol}^{-1}$)	0.20728 (544.20 $\text{kJ}\cdot\text{mol}^{-1}$)

The comparison of data in the Tables 1, 2 and 3 clearly shows that during the reaction the dissociation of the dihydrogen molecule of the homolytic type and the formation of the two C-H bonds intervened, on the one hand, and the MP2 chemical quantum calculation confirmed this hypothesis, on the other hand. In fact, the energy of the reaction obtained while we consider the catalytic sites (Tables 1 and 2) and the energy of the dissociation of H_2 and the formation of two C-H bonds are of the same order of magnitude as far as the MP2 calculation is considered.

On the basis of this study the reaction mechanism proposed for the hydrogenation of oxirene molecule is given in Scheme II.



Scheme II. Probable mechanism for the oxirene hydrogenation on $MoS_3H_3^+$ and $WS_3H_3^+$.

For this reaction, the formation of the oxirane the cyclic hydrogenated derivative of the oxirene is not favoured because of the ring strain. The relative energies of the oxirane ($E_{HF} = -152.81198$ a.u.) and acetaldehyde ($E_{HF} = -152.86919$ a.u.) confirm this chemical reality.

Otherwise, the gap between the highest occupied molecular orbital (HOMO) and the lowest unoccupied molecular orbital (LUMO) in the optimized adsorptive geometry of all the system is the same order of magnitude (-0.3462 a.u. on $MoS_3H_3^+$ and -0.3478 a.u. on $WS_3H_3^+$) which shows that the hydrogenation of oxirene can be carried out on these two catalytic sites indifferently.

CONCLUSIONS

The theoretical study carried out on the oxirene on the three anionic vacancies sites based upon the molybdenum and tungsten disulfide of $MoS_3H_3^+$ and $WS_3H_3^+$ type, respectively, has shown that the hydrogenation of this molecule pass through a dissociation process on the one hand, and the results obtained are comparable on the two catalytic sites, on the other hand. During the process, the breaking of the H-H bond and the formation of two C-H bonds are intervened. The results obtained with the MP2 calculation method confirmed this hypothesis. At last, the aliphatic product obtained after the hydrogenation of the oxirene has confirmed that the cyclic hydrogenated derivative of this molecule, the oxirane is less stable than the acetaldehyde molecule, its aliphatic isomer.

REFERENCES

1. Burch, R.; Collins, A. in *Proceedings, Climax 4th International Conference*, Golden, Colorado, Ann. Arbor, Michigan, **1982**; p. 379.
2. Vyskocin, V.; Tomanova, D. *React. Kinet. Catal. Lett.* **1979**, 10, 37.
3. Uchytel, J.; Beranek, L.; Zahrdnikova, H.; Kraus, M., *Appl. Catal.* **1982**, 4, 233.
4. Bodrero, T.A.; Bartholomew, C.H. *J. Catal.* **1983**, 84, 145.
5. Millman, W.S.; Hall, W.K. *J. Catal.* **1979**, 59, 311.
6. Lombardo, E.A.; Lojacano, M.; Hall, W.K. *J. Catal.* **1980**, 64, 150.
7. Hay, P.J.; Wadt, W.R. *J. Chem. Phys.* **1985**, 82, 470.
8. Becke, A.D. *J. Chem. Phys.* **1993**, 98, 5648.
9. Lee, C.; Yang, W.; Parr, R.G. *Phys. Rev.* **1980**, B37, 785.
10. Read Konings, A.J.A.; Brentjens, W.L.J.; Koningberger, D.C.; der Beer, V.H.J. *J. Catal.* **1981**, 67, 145.
11. Frisch, M.J.; Trucks, G.W.; Schlegel, H.B.; Scuseria, G.E.; Robb, M.A.; Cheeseman, J.R.; Zakrzewski, V.G.; Montgomery, J.A.; Stratmann, R.E.; Burant, J.C.; Dapprich, S.; Millam, J.M.; Daniels, A.D.; Kudin, K.N.; Strain, M.C.; Farkas, O.; Tomasi, J.; Barone, V.; Cossi, M.; Cammi, R.; Mennucci, B.; Pomelli, C.; Adamo, C.; Clifford, S.; Ochterski, J.; Petersson, G.A.; Ayala, P.Y.; Cui, Q.; Morokuma, K.; Malick, D.K.; Rabuck, A.D.; Raghavachari, K.; Foresman, J.B.; Cioslowski, J.; Ortiz, J.V.; Stefanov, B.B.; Liu, G.; Liashenko, A.; Piskorz, P.; Komaromi, I.; Gomperts, R.; Martin, R.L.; Fox, D.J.; Keith, T.; Al-Laham, M.A.; Peng, C.Y.; Nanayakkara, A.; Gonzalez, C.; Challacombe, M.; Gill, P.M.W.; Johnson, B.G.; Chen, W.; Wong, M.W.; Andres, J.L.; Head-Gordon, M.; Replogle, E.S.; Pople, J.A., *Gaussian 98 (Revision A.1)*, Gaussian Inc.: Pittsburgh PA. **1998**.
12. Vrinat, M.; Breyse, M.; Frety, R. *Appl. Catal.* **1984**, 12, 151.
13. Breyse, M.; Frety, R.; Vrinat, M.; Grange, P.; Genet, M. *Appl. Catal.* **1984**, 12, 165.
14. Topsøe, H.; Clausen, V.S.; Massoth, F.E., in *Hydrotreating Catalysis, Sciences and Technology*, Anderson, J.R.; Boudart, M. (Eds.), Springer, Berlin, **1996**.
15. Voorhoeve, R.J.H.; Stuiiver, J.C.M. *J. Catal.* **1971**, 23, 243.
16. Massoth, F.E.; Kibby, C.L. *J. Catal.* **1977**, 47, 300.
17. Schuit, G.C.A. *Int. J. Quant. Chem.* **1977**, 24, 43.
18. Anderson, A.B.; Al-Saigh, Z.Y.; Hall, W.K. *J. Phys. Chem.* **1988**, 92, 803.
19. Rodriguez, J.A., *J. Phys. Chem.* **1997**, B101, 7524.
20. Sierraalta, A.; Ruette, F.; Machado, E. *Int. J. Quantum Chem.* **1998**, 70, 113.
21. Joffre, J.; Lerner, D.A.; Geneste, P. *J. Catal.* **1986**, 97, 543.
22. Hoffmann, R. *J. Chem. Phys.* **1963**, 39, 1937.
23. Ahmetov, N.S. *Obchaya u Neorganitsheskaya Himia*, Vichaya Chkola, (Ed.), A.A. Jdanov Press: Moscow; **1988**; p 521.
24. Rubin, Y.; Kahr, M.; Knobler, C.B.; Diederich, F.; Wilkins, C.L. *J. Am. Chem. Soc.* **1991**, 113, 495.
25. Li, G.; Chang, H.T.; Sharpless, K.B., *Angew. Chem. Int. Ed. Engl.* **1996**, 35, 451.
26. Hill, W.; Miessner, H.; Öhlmann, G. *J. Chem. Soc. Faraday Trans. I* **1989**, 85, 691.
27. Pestman, R.; Koster, R.M.; Pieterse, J.A.Z.; Ponec, V. *J. Catal.* **1997**, 168, 255.